Journal for Geometry and Graphics
Volume 21 (2017), No. 2, 179–192.

Geometry and Design of Hexagonal Spirals (Voronoi and other)

Kostantinos Myrianthis

58, Zan Moreas street, Athens, P.C. 15231, Greece
email: myrian@ath.forthnet.gr

Abstract. The geometry of equiangular spirals, i.e., discretized logarithmic spirals, never ceases to attract interest in the broad mathematical world where professionals and amateurs belong to [1]. Voronoi and general hexagonal spiral systems have the unique attraction of offering opportunities for research with interesting results in geometry as well as in botany. The aim of the present work is to study the geometrical characteristics of such systems using synthetic and analytic methods.

Key Words: spiral system, spiral phyllotaxis, quadrangular spiral system, hexagonal spiral system, Voronoi tiling, Voronoi cell, Delaunay triangulation

MSC 2010: 51M04, 51N20, 97M60

1. Introduction

In the sequel the term *spiral* stands for the orbit $A_0A_1A_2\dots$ of a point under iterations of a stretch-rotation, which is the commutative product of a dilatation with factor $\kappa \leq 1$ and a rotation with the same center S through the signed angle $\widehat{\phi}$, where $0 < |\widehat{\phi}| < \pi$. If we apply a second stretch-rotation with the same center, but different factor $\lambda \leq 1$ and signed angle $\widehat{\theta}$ with $0 < |\widehat{\phi}| < \pi$ we obtain a *spiral system* $A_{0,0}A_{1,0}A_{2,0}\dots$, $A_{0,1}A_{1,1}A_{2,1}\dots$, $A_{0,2}A_{2,1}\dots$. The orbits of the two defining stretch-rotations are called *branches* of the system or, more precisely, κ-branches and λ-branches.

In botany, such systems are known as *spiral phyllotaxis*. Relevant mathematical models for Voronoi spirals (or tilings) are presented in [7]. In [2] a series of synthetic and analytic properties in the phyllotaxis context is provided. In the present work, the synthetic and analytical approach of [3] is extended to Voronoi and other hexagonal spirals.

We can generate a spiral system also by applying the stretch-rotations to the quadrangle $A_{0,0}A_{1,0}A_{1,1}A_{1,1}$, called a *defining quadrangle*. Thus we obtain a quadrangular net consisting of similar quadrangles. It is called a *quadrangular spiral system*. In Figures 1, 2, 3, 4, and 5 typical examples of quadrangular spiral systems are shown. Our notation of parameters and the numbering follows [3]. This means

$$\kappa = A_{i,1}S/A_{i,0}S = A_{i,2}S/A_{i,1} = \cdots, \quad \widehat{\phi} = \widehat{A_{i,0}SA_{i,1}} = \widehat{A_{i,1}SA_{i,2}} = \cdots \quad \text{for } i = 0, 1, 2, \dots$$

ISSN 1433-8157/$ 2.50

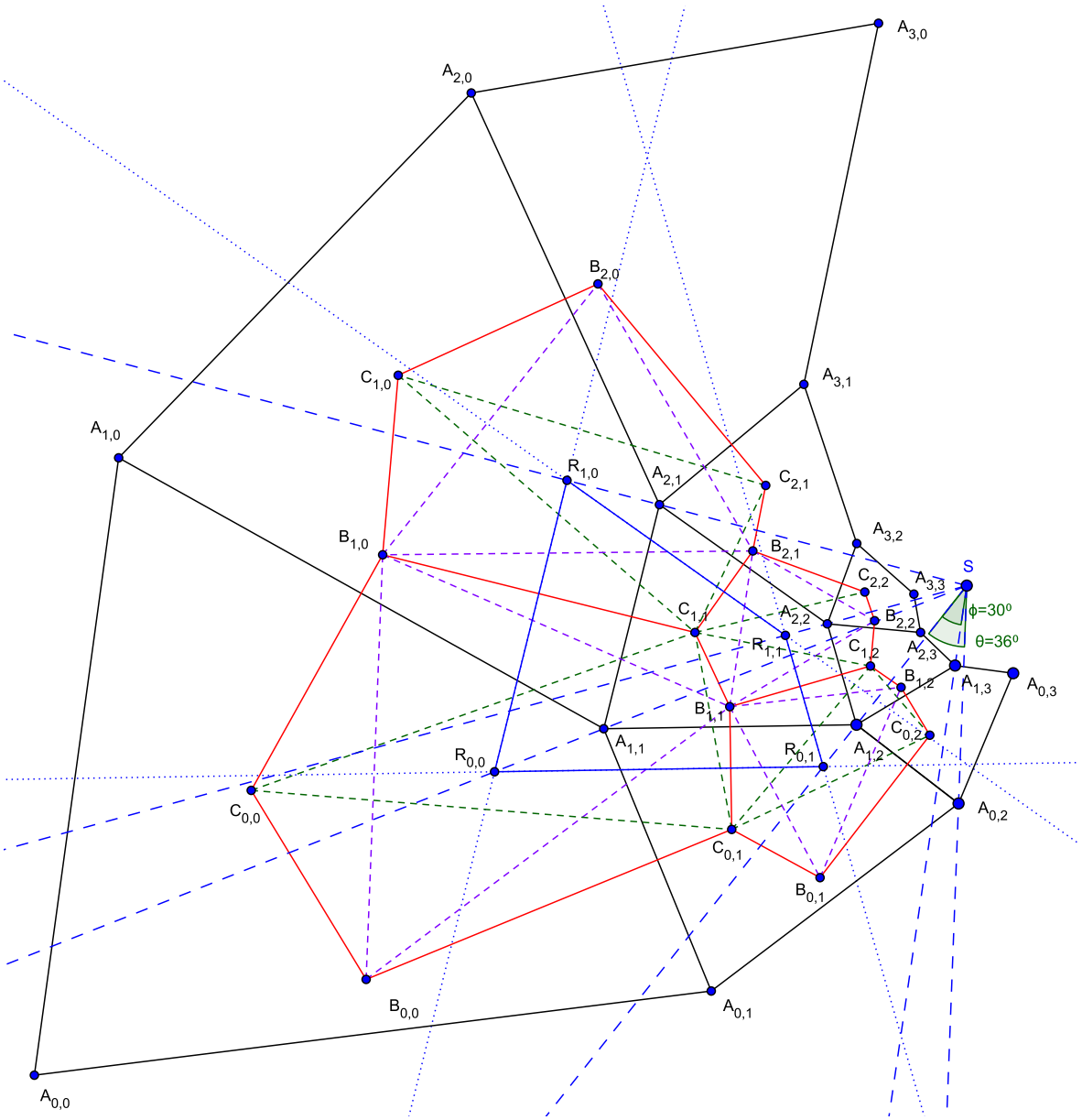

Figure 1: Quadrangular spiral system and Voronoi hexagonal spiral system

and

$$\lambda = A_{1,j}S/A_{0,j}S = A_{2,j}S/A_{1,j} = \cdots, \quad \widehat{\phi} = \widehat{A_{0,j}SA_{1,j}} = \widehat{A_{1,j}SA_{2,j}} = \cdots \quad \text{for } j = 0, 1, 2, \ldots$$

It is a well-known property of orientation-preserving similarities that the angles also show up as angles between corresponding directed line segments:

$$\begin{aligned} \angle \overrightarrow{A_{i,0}A_{i,1}}\,\overrightarrow{A_{i,1}A_{i,2}} &= \angle \overrightarrow{A_{i,1}A_{i,2}}\,\overrightarrow{A_{i,2}A_{i,3}} = \cdots = \widehat{\phi} \quad \text{and} \\ \angle \overrightarrow{A_{0,j}A_{1,j}}\,\overrightarrow{A_{1,j}A_{2,j}} &= \angle \overrightarrow{A_{1,j}A_{2,j}}\,\overrightarrow{A_{2,j}A_{3,j}} = \cdots = \widehat{\theta} \end{aligned} \tag{1}$$

(see also [3]). In Figures 1 and 2 $\widehat{\phi}$ is positive, i.e., the corresponding stretch-rotation $A_{i,0} \mapsto A_{i,1}$ anti-clockwise, and $\widehat{\theta}$ negative, the stretch-rotation $A_{0,j} \mapsto A_{1,j}$ clockwise.

A quadrangular spiral system is called *closed* if there are $m, n \in \mathbb{N}$ such that

$$n|\widehat{\theta}| \mp m|\widehat{\phi}| = 2\pi \quad \text{and} \tag{2}$$

$$\lambda^n = \kappa^m. \tag{3}$$

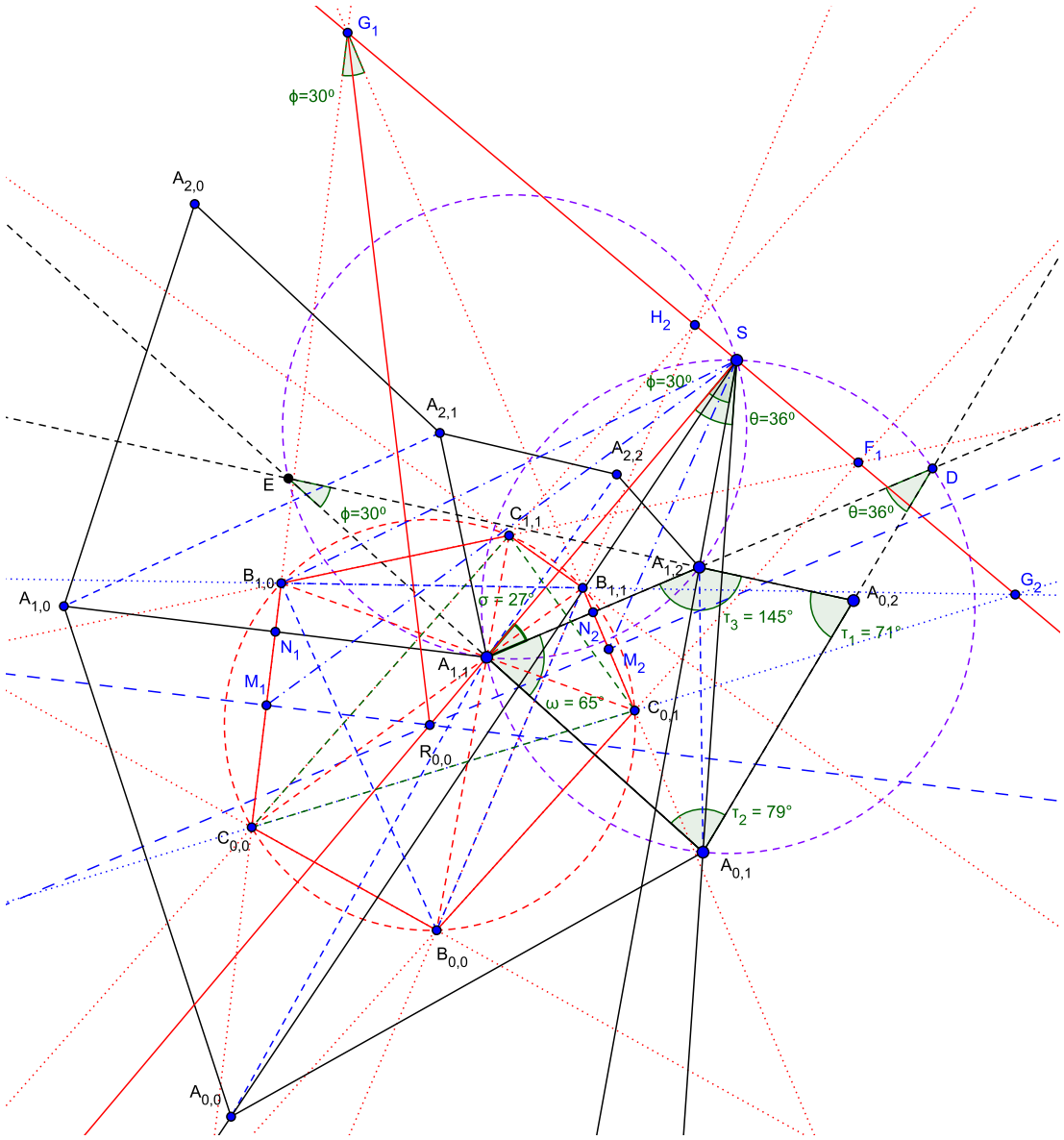

Figure 2: Typical cyclic Voronoi hexagon and its V-line

If the sign in (2) is negative the branches *co-rotate;* otherwise they *contra-rotate*. We say $(\widehat{\phi}, \kappa, \widehat{\theta}, \lambda, n, m)$ are the parameters of this system.

A *hexagonal Voronoi spiral system* can be produced from a quadrangular spiral system by applying the Delaunay triangulation to the quadrangles, as seen in Figure 2. We insert the diagonal which connects vertices whose sum of interior angles is $\geq \pi$. For example, in Figure 2 the diagonal $A_{0,0}A_{1,1}$ is a *Delaunay edge* (see [7]). This diagonal separates the defining quadrangle into the triangles $\triangle A_{0,0}A_{0,1}A_{1,1}$ and $\triangle A_{0,0}A_{1,0}A_{1,1}$. Now we define point $B_{0,0}$ as circumcenter of the first triangle and $C_{0,0}$ as circumcenter of second.

After applying iteratively the given stretch-rotations, we obtain centers $B_{i,j}$ of triangles similar to $\triangle A_{0,0}A_{0,1}A_{1,1}$ and centers $C_{i,j}$ of triangles similar to $\triangle A_{0,0}A_{1,0}A_{1,1}$. For this triangulation, the circumcenters of all triangles sharing the vertex $A_{1,1}$ define the hexagon $B_{0,0}C_{0,0}B_{1,0}C_{1,1}B_{1,1}C_{0,1}$ whose sides are respectively the orthogonal bisectors of the edges through $A_{1,1}$. This hexagon bounds the *Voronoi cell* of $A_{1,1}$ with respect to our spiral system.

As shown in Figure 1, the transformed hexagons form a hexagonal net.

In Sections 2 and 3, the properties of hexagonal spirals (Voronoi or not) are presented. In Section 4 it is proven that there is no spiral system with polygons with a number of sides higher than six.

2. Voronoi hexagonal spirals and properties

A mathematical description based on complex numbers and properties for Voronoi spiral systems can be found in [7]. In [2] it is shown that for a given set of points different spirals can be defined. In the present work, we provide a study of the properties of any given set of spiral points plus an enhanced list of properties of Voronoi systems, and we put emphasis on how these spiral points affect the produced hexagonal spirals.

One of these properties is that the transition of the Voronoi hexagons into quadrangles (Figure 3) is only possible when the branches of the defining quadrangles contra-rotate and the defining quadrangles have a circumcircle, i.e., they are *cyclic* ([7], Appendix). The Figures 3, 4 and 5 show three possibilities of Voronoi quadrangles:

a) Figure 3: $C_{1,1} \equiv B_{1,1}$ (= circumcentre of $\square A_{1,1}A_{1,2}A_{2,2}A_{2,1}$) and $C_{0,0} \equiv B_{0,0}$, since the branches of the given spiral system contra-rotate.

b) Figure 4: $C_{0,1} \equiv B_{1,1}$ (= circumcentre of alternative $\square A_{1,1}A_{0,1}A_{1,2}A_{2,2}$) and $C_{0,0} \equiv B_{1,0}$. This condition can take place either when the branches of the given spiral system co-rotate if $|\widehat{\phi}| < |\widehat{\theta}|$, or when they contra-rotate if $|\widehat{\phi}| > |\widehat{\theta}|$. If $|\widehat{\phi}| = |\widehat{\theta}|$ and $\lambda = 1$ then $C_{0,1} \equiv B_{1,1}$ and $C_{0,0} \equiv B_{1,0}$ for all κ.

c) Figure 5: $C_{1,1} \equiv B_{1,0}$ (= circumcentre of alternative $\square A_{1,1}A_{1,0}A_{2,1}A_{2,2}$) and $C_{0,1} \equiv B_{0,0}$. If $|\widehat{\phi}| = |\widehat{\theta}|$ and $\kappa = 1$ then $C_{1,1} \equiv B_{1,0}$ and $C_{0,1} \equiv B_{0,0}$ for all λ.

For given $\widehat{\phi}$, $\widehat{\theta}$ and $\square A_{1,1}A_{0,1}A_{0,2}A_{1,2}$, if $A_{1,1}$ and $A_{1,2}$ remain constant and $A_{0,1}$ moves along the ray $SA_{0,1}$, then the points $A_{0,2}$ and $A_{2,2}$ move respectively along the rays $SA_{0,2}$ and $SA_{2,2}$ (note $\widehat{A_{1,2}SA_{0,2}} = \widehat{A_{2,2}SA_{1,2}} = \widehat{\theta}$). So $B_{1,1}$ and $C_{0,1}$ converge until they coincide (second possibility). Also, $B_{1,1}$ and $C_{1,1}$ can converge until they coincide (first possibility, if the defining branches contra-rotate and $|\widehat{\phi}| < |\widehat{\theta}|$). Similarly we can get the third possibility. By variation of one vertex the solution will always be bound by a combination of two of the three possibilities.

Based on the possibilities b) and c), as given above, there is an alternative set of α-branches $A_{0,0}A_{1,1}A_{2,2}\ldots$, $A_{1,0}A_{2,1}\ldots$, etc. with dilation factor α and clockwise ($|\widehat{\theta}| > |\widehat{\phi}|$) or anticlockwise ($|\widehat{\theta}| < |\widehat{\phi}|$) rotation. The combination with the λ-branches creates the alternative spiral system of the possibility b) (Figure 4). When combined with the κ-branches, we obtain the alternative spiral system of possibility c) (Figure 5). Since $|\widehat{\theta}| > |\widehat{\phi}|$, we get: in the Figures 1, 2, 3, and 5, where the λ-branches rotate clockwise and the κ-branches anticlockwise, we have $\alpha = \kappa\lambda$. In Figure 4, where λ- and κ-branches rotate anticlockwise, we have $\alpha = \kappa/\lambda$.

As can be seen in Figure 4, $\square A_{1,1}A_{0,1}A_{1,2}A_{2,2}$ has a circumcircle only when the α- and λ-branches contra-rotate. This is possible only when either the branches of the given spiral system co-rotate and $|\widehat{\phi}| < |\widehat{\theta}|$ (the α- and λ-branches contra-rotate), or, when the branches of the given spiral system contra-rotate and $|\widehat{\phi}| > |\widehat{\theta}|$ (the α- and λ-branches contra-rotate, because they both change orientation), assuming in these two cases that the κ-branches keep the same orientation. (There is a duality, $\widehat{\phi} \leftrightarrow \widehat{\theta}$ and $\kappa \leftrightarrow \lambda$, note Lemma 4.) The case, where

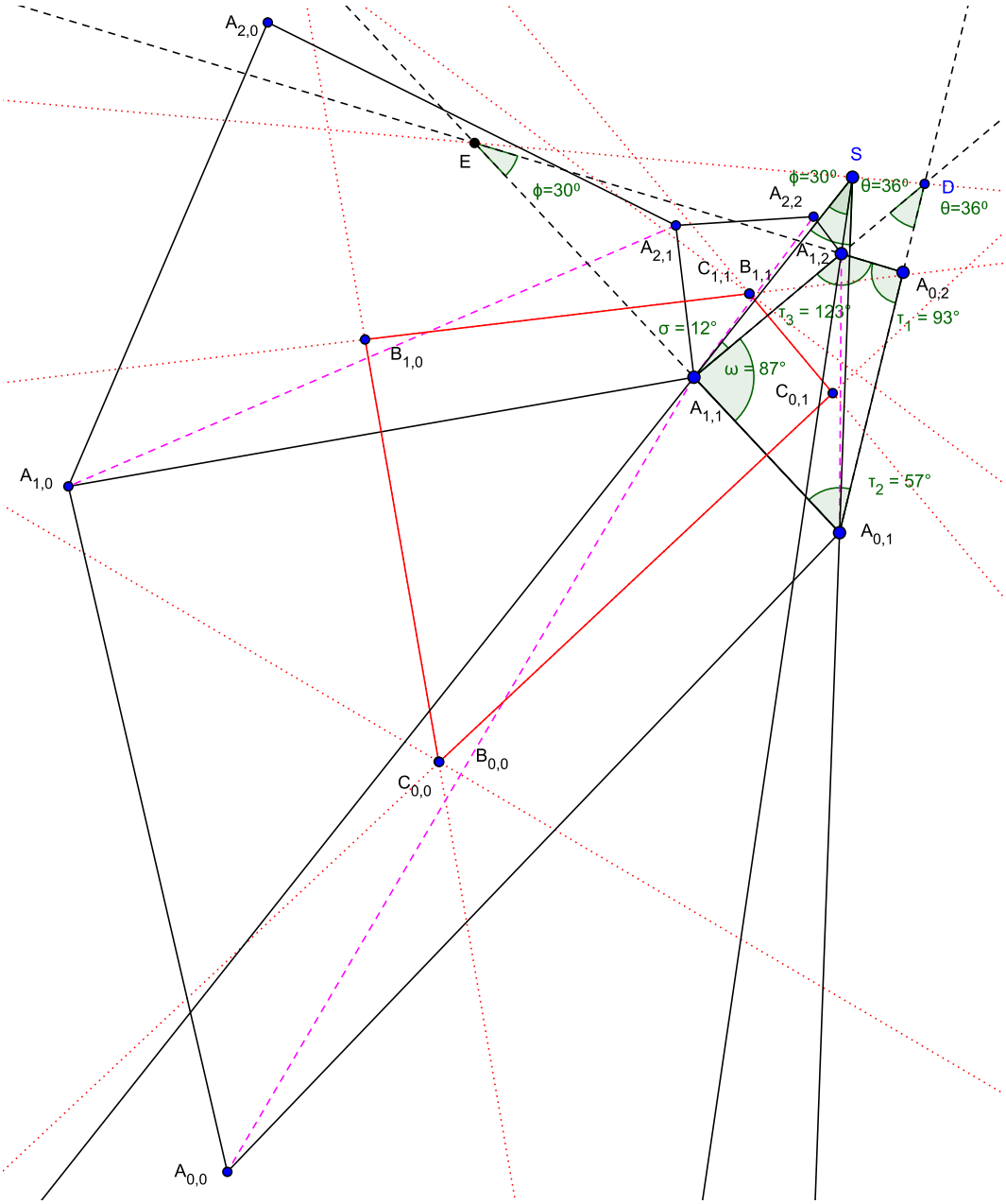

Figure 3: Quadrangular spiral system with cyclic quadrangles and a Voronoi quadrangle

$|\widehat{\phi}| < |\widehat{\theta}|$ and the branches of the given spiral system contra-rotate, is related to the third possibility. As can be seen in Figure 5, $\square A_{0,0}A_{0,1}A_{1,2}A_{1,1}$ has a circumcircle only when the α- and κ-branches contra-rotate. This is possible when $|\widehat{\phi}| < |\widehat{\theta}|$ and either the branches of the given spiral system co-rotate or contra-rotate, as long as the α- and κ-branches contra-rotate, assuming that the κ-branches keep the same rotation.

All the above constitutes the proof of the following

Lemma 1. *For any given spiral system, formed by the κ- and λ-branches$A_{i,0}A_{i,1}A_{i,2}\ldots$ and $A_{0,j}A_{1,j}A_{2,j}\ldots$, we can define an alternative set of α-branches $A_{0,0}A_{1,1}A_{2,2}\ldots$, $A_{1,0}A_{2,1}\ldots$, etc. where the endpoints of the Delaunay edges (such as $A_{0,1}\mapsto A_{1,2}$ in $\square A_{0,1}A_{0,2}A_{1,2}A_{1,1}$) are corresponding under the related stretch-rotation.*

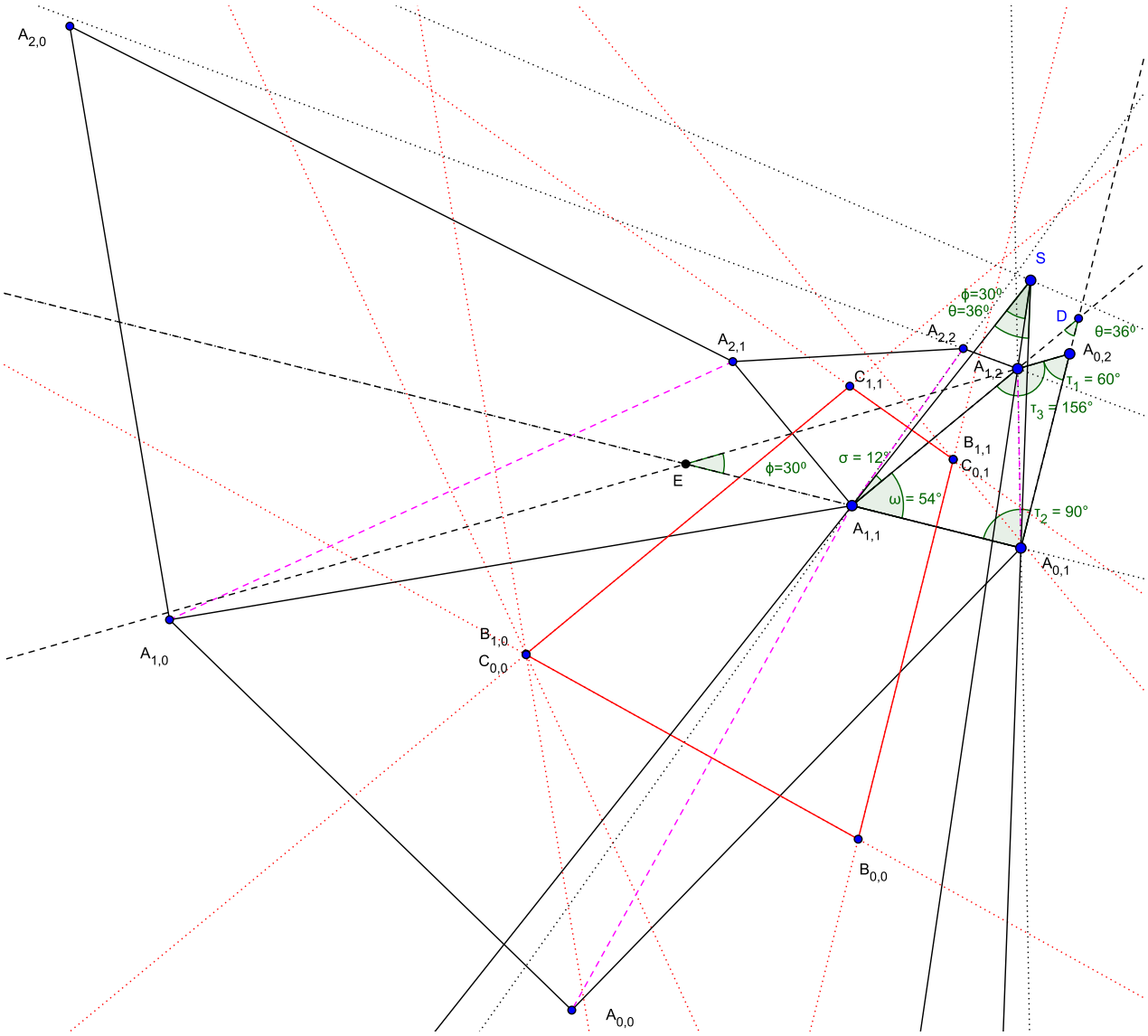

Figure 4: Cyclic alternative λ-spiral system and Voronoi quadrangles

Lemma 2. *The combination of the alternative α-branches, as introduced in Lemma 1, with the λ-branches $A_{0,j}A_{1,j}A_{2,j}A_{3,j}\ldots$ creates the 'alternative λ-spiral system' with defining quadrangles $\square A_{0,0}A_{1,0}A_{2,1}A_{1,1}$, etc.*

Lemma 3. *The combination of the alternative α-branches from Lemma 1 with the κ-branches $A_{i,0}A_{i,1}A_{i,2}A_{i,3}\ldots$ creates the 'alternative κ-spiral system' with defining quadrangles $\square A_{0,0}A_{0,1}A_{1,2}A_{1,1}$, etc.*

Theorem 1. *There are three cases of quadrangular spiral systems, where the Voronoi hexagons become quadrangles:*

a. the defining quadrangles of the given spiral system (see $\square A_{1,1}A_{0,1}A_{0,2}A_{1,2}$ in Figure 3) are cyclic only, when the defining branches contra-rotate.

b. the defining quadrangles of the alternative λ-spiral system (see $\square A_{1,1}A_{0,1}A_{1,2}A_{2,2}$ in Figure 4) are cyclic, when the α- and λ-branches contra-rotate and either the defining branches co-rotate if $|\widehat{\phi}| < |\widehat{\theta}|$ or contra-rotate if $|\widehat{\phi}| > |\widehat{\theta}|$ (duality in $\widehat{\phi} \leftrightarrow \widehat{\theta}$ and $\kappa \leftrightarrow \lambda$).

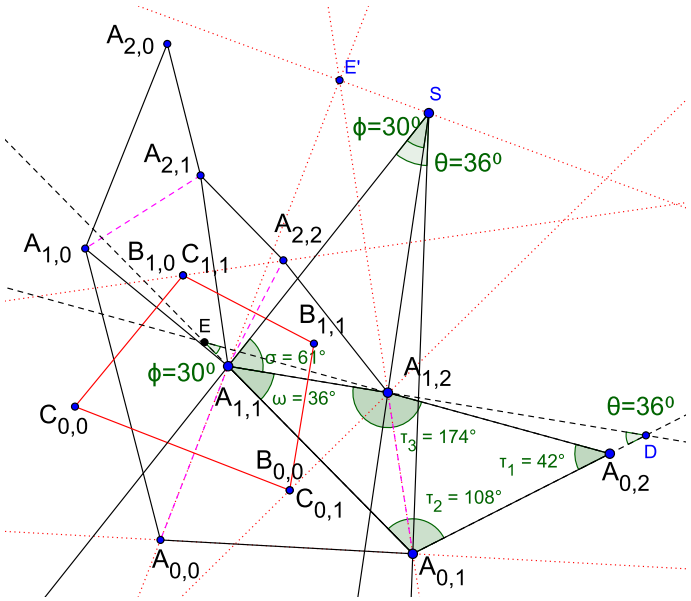

Figure 5: Cyclic alternative κ-spiral system and a Voronoi quadrangle

c. the defining quadrangles of the alternative κ-spiral system (see $\square A_{0,0}A_{0,1}A_{1,2}A_{1,1}$ in Figure 5) are cyclic, when the α- and κ-branches contra-rotate and the defining branches either contra-rotate or co-rotate.

It is known that, in the sense of graph theory, the Delaunay tessellation is dual to the Voronoi tiling [7], and this can be further extended in spiral systems as follows:

Lemma 4. *The alternative λ- and κ-spiral systems are duals of the defining spiral system, since one system is derived from the other by inserting the Delaunay edges in every quadrangle of the other system. For closed spiral systems the parameters $\widehat{\phi}$, κ, m are duals of $\widehat{\theta}$, λ, n (Eqs. (2) and (3)).*

Given $\widehat{\phi}$, n, m, we can calculate $\widehat{\theta}$ from Eq. (2). According to [3], following the notation in Figures 2–5, we have

$$\tan(\widehat{\omega}+\widehat{\sigma}) = \lambda \sin|\widehat{\theta}|/(1-\lambda\cos\widehat{\theta}), \quad \tan\widehat{\sigma} = \kappa\sin|\widehat{\phi}|/(1-\kappa\cos\widehat{\phi}),$$

and solving for λ we obtain

$$\lambda = \frac{\sin|\widehat{\theta}| + \tan\widehat{\omega}\cos\widehat{\theta} - \kappa(\sin(|\widehat{\theta}|-|\widehat{\phi}|) + \tan\widehat{\omega}\cos(|\widehat{\theta}|-|\widehat{\phi}|))}{\tan\widehat{\omega} - \kappa(\tan\widehat{\omega}\cos\widehat{\phi} - \sin|\widehat{\phi}|)}.$$

Also from [3] and from Figure 2 we have $\widehat{\tau_1} = \widehat{A_{1,2}A_{0,2}}A_{0,1} = \widehat{\omega} + |\widehat{\theta}| - |\widehat{\phi}|$, and if the condition $\widehat{A_{1,2}A_{1,1}}A_{0,1} + A_{1,2}\widehat{A_{0,2}A_{0,1}} = \pi$ holds we obtain $\widehat{\omega} = (\pi + |\widehat{\phi}| - |\widehat{\theta}|)/2$, hence $\tan\widehat{\omega} = 1/\tan\dfrac{(|\widehat{\theta}|-|\widehat{\phi}|)}{2}$.

Since $\tan\widehat{(x/2)} = \sin\widehat{x}/(1+\cos\widehat{x})$, we derive from all the above

$$\lambda = \frac{\cos\widehat{\phi} + \cos\widehat{\theta} - \kappa(1+\cos(|\widehat{\theta}|-|\widehat{\phi}|))}{1+\cos(|\widehat{\theta}|-|\widehat{\phi}|) - \kappa(\cos\widehat{\phi}+\cos\widehat{\theta})}.$$

The parameter κ is in inverse variation with respect to λ in the above equation. Also from Eq. (2) we get that the parameter κ is in direct variation with respect to λ. So from these two relations, since $\lambda \in [0,1]$ and $\kappa \in [0,1]$, we always get a solution with λ and κ satisfying (2) and the above equation. We notice in the above equation that for $\kappa = 0$

$$\lambda = [\cos\widehat{\phi} + \cos\widehat{\theta}]/[1 + \cos(|\widehat{\theta}| - |\widehat{\phi}|)] < 1,$$

and for $\lambda = 0$

$$\kappa = [\cos\widehat{\phi} + \cos\widehat{\theta}]/[1 + \cos(|\widehat{\theta}| - |\widehat{\phi}|)] < 1.$$

This implies

Lemma 5. *Given $\widehat{\phi}$, n, m of a closed defining quadrangular spiral system, we can always calculate $\widehat{\theta}$, κ and λ in order to obtain cyclic defining quadrangles.*

As displayed in Figures 1 and 2, each vertex of the hexagon $B_{0,0}C_{0,0}B_{1,0}C_{1,1}B_{1,1}C_{0,1}$ is the circumcenter of a triangle in the triangulation. The stretch-rotation with factor λ maps $\square A_{0,1}A_{1,1}A_{1,2}A_{0,2}$ onto $\square A_{1,1}A_{2,1}A_{2,2}A_{1,2}$. Therefore $\widehat{\theta} = \widehat{C_{0,1}SC_{1,1}}$, and similarly $\widehat{\phi} = \widehat{C_{0,0}SC_{0,1}}$. Consequently we get $\widehat{C_{0,0}SC_{1,1}} = \widehat{\theta} + \widehat{\phi}$, $\widehat{B_{0,0}SB_{1,0}} = \widehat{\theta}$, $\widehat{B_{1,0}SB_{1,1}} = \widehat{\phi}$ and $\widehat{B_{0,0}SB_{1,1}} = \widehat{\theta} + \widehat{\phi}$ (note in Figures 1 and $2\widehat{\phi} > 0$, $\widehat{\theta} < 0$ and $|\widehat{\theta}| > |\widehat{\phi}|$). From all the above, we get the following:

Lemma 6. *At the Voronoi hexagon $B_{0,0}C_{0,0}B_{1,0}C_{1,1}B_{1,1}C_{0,1}$ (see Figure 1) and similarly at its images under the stretch-rotations we recognize:*

a. Triangle $\triangle C_{0,0}C_{1,1}C_{0,1}$: $\widehat{C_{0,1}SC_{1,1}} = \widehat{\theta}$, $\widehat{C_{0,0}SC_{0,1}} = \widehat{\phi}$ and $\widehat{C_{0,0}SC_{1,1}} = \widehat{\theta} + \widehat{\phi}$.

b. Triangle $\triangle B_{0,0}B_{1,0}B_{1,1}$: $\widehat{B_{0,0}SB_{1,0}} = \widehat{\theta}$, $\widehat{B_{1,0}SB_{1,1}} = \widehat{\phi}$ and $\widehat{B_{0,0}SB_{1,1}} = \widehat{\theta} + \widehat{\phi}$.

c. The sides of these triangles define six spiral branches per hexagon (Figures 1, 2):
c1. $C_{0,1}C_{1,1}C_{2,1}\ldots$ and $B_{0,0}B_{1,0}B_{2,0}\ldots$ are two λ-branches .
c2. $C_{0,0}C_{0,1}C_{0,2}\ldots$ and $B_{1,0}B_{1,1}B_{1,2}\ldots$ are two κ-branches.
c3. $C_{0,0}C_{1,1}C_{2,2}\ldots$ and $B_{0,0}B_{1,1}B_{2,2}\ldots$ are α-branches.

d. From c1 and c2 we get two quadrangles, $\square C_{0,1}C_{1,1}C_{1,2}C_{0,2}$ and $\square B_{1,1}B_{2,1}B_{2,2}B_{1,2}$ which define separate spiral system with quadrangles similar to the given $\square A_{0,0}A_{1,0}A_{1,1}A_{0,1}$.

The defining quadrangle $\square A_{0,0}A_{1,0}A_{1,1}A_{0,1}$ of our quadrangular spiral system is split by the Delaunay edge into two triangles with respective circumcenters $B_{0,0}$ and $C_{0,0}$ (see Figure 2). We connect these centers with the vertices of the corresponding triangles and obtain isosceles subtriangles with congruent signed interior base angles, which we denote as given below:

$$\begin{aligned}
\widehat{O_1} &= A_{0,0}\widehat{A_{1,1}B_{0,0}} = B_{0,0}\widehat{A_{0,0}A_{1,1}}, \quad & \widehat{O_2} &= A_{1,1}\widehat{A_{0,0}C_{0,0}} = C_{0,0}\widehat{A_{1,1}A_{0,0}},\\
\widehat{O_3} &= A_{1,0}\widehat{A_{1,1}C_{0,0}} = C_{0,0}\widehat{A_{1,0}A_{1,1}}, \quad & \widehat{O_4} &= A_{0,0}\widehat{A_{1,0}C_{0,0}} = C_{0,0}\widehat{A_{0,0}A_{1,0}},\\
\widehat{O_5} &= A_{1,1}\widehat{A_{0,1}B_{0,0}} = B_{0,0}\widehat{A_{1,1}A_{0,1}}, \quad & \widehat{O_6} &= A_{0,1}\widehat{A_{0,0}B_{0,0}} = B_{0,0}\widehat{A_{0,1}A_{0,0}},
\end{aligned} \tag{4}$$

where $-\frac{\pi}{2} < \widehat{O_i} < \frac{\pi}{2}$. Of course,

$$\widehat{O_2} + \widehat{O_3} + \widehat{O_4} = \widehat{O_5} + \widehat{O_6} + \widehat{O_1} = \frac{\pi}{2}\,.$$

All angles remain the same when at each involved point the first subscript is increased by 1; and this can be iterated. The same holds for the second subscripts.

With this observation we will be able to prove the following

Theorem 2. *Each Voronoi hexagon of a given quadrangular spiral system, as displayed in Figures 1 and 2, has the following properties:*

a. *The three main diagonals meet at a point which is a quadrangle's vertex inside the hexagon.*
b. *The hexagon has a circumcircle.*
c. *For any spiral system with a cyclic defining quadrangle ($\square A_{1,1}A_{0,1}A_{0,2}A_{1,2}$ in Figure 3) the Voronoi hexagons become quadrangles, too (Theorem 1a). For each quadrangle of the spiral system the intersection points of the two pairs of opposite sides are collinear with S, the centre of the spiral system. This line (ESD in Figure 3) can be called* cyclic spiral line. *Analogue results hold for the cases of Theorems 1b and 1c.*
d. *At each Voronoi hexagon the intersection points of the three pairs of opposite sides are collinear with the center S of the spiral system. This line can be called* V-line *of the hexagon ('V' stands for Voronoi). Also the pairs of opposite diagonals meet on this line (see Figure 2). This line is polar with respect to the circumcircle to the quadrangle's vertex inside the hexagon. The center S is the pedal point of the V-line with respect to this vertex.*

Proof. **a.** Using the notation defined in Eq. (4), we calculate

$$\begin{aligned} B_{1,0}\widehat{A_{1,1}C_{0,1}} &= B_{1,0}\widehat{A_{1,1}A_{1,0}} + A_{1,0}\widehat{A_{1,1}A_{0,0}} + A_{0,0}\widehat{A_{1,1}A_{0,1}} + A_{0,1}\widehat{A_{1,1}C_{0,1}} \\ &= \widehat{O_6} + (\widehat{O_3} + \widehat{O_2}) + (\widehat{O_1} + \widehat{O_5}) + \widehat{O_4} = \pi. \end{aligned}$$

So, the points $B_{1,0}$, $A_{1,1}$ and $C_{0,1}$ are collinear. Similarly we can prove that also the points $C_{0,0}$, $A_{1,1}$ and $B_{1,1}$ are collinear as well as the points $B_{0,0}$, $A_{1,1}$ and $C_{1,1}$. Thus, the main diagonals share the vertex $A_{1,1}$.

b. From Figure 2 we get $A_{1,1}\widehat{B_{1,0}C_{0,0}} = \frac{\pi}{2} - \widehat{O_6}$, $A_{1,1}\widehat{B_{1,0}C_{1,1}} = \frac{\pi}{2} - \widehat{O_5}$ and $C_{1,1}\widehat{B_{1,1}A_{1,1}} = \frac{\pi}{2} - \widehat{O_1}$. At the quadrangle $\square C_{1,1}B_{1,1}C_{0,0}B_{1,0}$ the sum of the opposite angles is

$$C_{1,1}\widehat{B_{1,1}C_{0,0}} + C_{0,0}\widehat{B_{1,0}C_{1,1}} = \frac{\pi}{2} - \widehat{O_1} + \pi - (\widehat{O_5} + \widehat{O_6}) = \frac{3\pi}{2} - \widehat{O_5} - \widehat{O_6} - \widehat{O_1} = \pi.$$

Therefore the quadrangle $\square C_{1,1}B_{1,1}C_{0,0}B_{1,0}$ is cyclic.
Similarly we can prove that the quadrangles $\square C_{1,1}B_{1,1}C_{0,1}B_{1,0}$, $\square C_{1,1}B_{1,1}C_{0,1}B_{0,0}$, $\square B_{1,1}C_{0,1}B_{0,0}C_{0,0}$, $\square C_{0,1}B_{0,0}C_{0,0}B_{1,0}$, and $\square B_{0,0}C_{0,0}B_{1,0}C_{1,1}$ are cyclic. So the Voronoi hexagon $B_{0,0}C_{0,0}B_{1,0}C_{1,1}B_{1,1}C_{0,1}$ is cyclic.

c. Let E denote the point of intersection of $A_{0,1}A_{1,1}$ and $A_{0,2}A_{1,2}$, and D denote the intersection of $A_{0,1}A_{0,2}$ and $A_{1,1}A_{1,2}$. In Figure 3 we notice that $\square EA_{1,1}A_{1,2}S$ is cyclic since $A_{1,1}\widehat{SA}_{1,2} = A_{1,1}\widehat{EA}_{1,2} = \widehat{\phi}$ (see [3]). Similarly, $\square SA_{1,2}A_{0,2}D$ is cyclic, because $A_{0,2}\widehat{SA}_{1,2} = A_{0,2}\widehat{DA}_{1,2} = \widehat{\theta}$ (see [6]), and $\square A_{1,1}A_{0,1}A_{0,2}A_{1,2}$ is cyclic, because we have the conditions of a Voronoi quadrangle, by virtue of Theorem 1a (Figure 3). Therefore $\widehat{A_{1,2}SD} + D\widehat{A_{0,2}A_{1,2}} = \pi$, $\widehat{ESA_{1,2}} + A_{1,2}\widehat{A_{1,1}E} = \pi$, furthermore $\widehat{ESA_{1,2}} = \pi - A_{1,2}\widehat{A_{1,1}E} = A_{0,1}\widehat{A_{1,1}A_{1,2}} = D\widehat{A_{0,2}A_{1,2}}$, hence

$$\widehat{A_{1,2}SD} + \widehat{ESA_{1,2}} = \pi - D\widehat{A_{0,2}A_{1,2}} + D\widehat{A_{0,2}A_{1,2}} = \pi.$$

This means that E, D and S are collinear.
Similarly the case of Theorem 1b (Figure 4 with the cyclic quadrangle $\square A_{0,0}A_{1,1}A_{2,1}A_{1,0}$) can be treated as well as that of Theorem 1c (Figure 5 with the cyclic $\square A_{0,0}A_{0,1}A_{1,2}A_{1,1}$).

d. A standard result of Projective Geometry states that, due to item a, the pairs of opposite points of the Voronoi hexagon define a perspective collineation which maps the circumcircle onto itself. The common point of the main diagonals ($A_{1,1}$ in Figure 2) is the center of this collineation and its polar line with respect to the circumcircle is the axis, called V-line. Pairs of corresponding lines like opposite sides or diagonals intersect on the axis.
It remains to show, that also the center S of the spiral system lies on the axis. We refer to Figure 2 and denote with G_1 the intersection of the sides $C_{0,0}B_{1,0}$ and $C_{0,1}B_{1,1}$. Point G_2 is the intersection of $B_{1,0}B_{1,1}$ and $C_{0,0}C_{0,1}$.
The quadrangle $\square C_{0,0}B_{1,0}B_{1,1}C_{0,1}$ in Figure 2 is cyclic, and $\widehat{B_{1,0}SB_{1,1}} = \widehat{C_{0,0}SC_{0,1}} = \widehat{\phi}$ by Lemma 6c2. By Eq. (1) we have $\widehat{\phi} = \angle\overrightarrow{C_{0,0}B_{1,0}}\,\overrightarrow{C_{0,1}B_{1,1}}$ and $\widehat{C_{0,0}SB_{1,0}} = \widehat{C_{0,1}SB_{1,1}}$, as shown in Figures 1 and 2. In Figure 1, we have the spiral branches of Lemmas 6c1, 6c2 and 6c3, therefore by (1) $\widehat{C_{0,0}SB_{1,0}} = \angle\overrightarrow{B_{1,0}B_{1,1}}\,\overrightarrow{C_{0,0}C_{0,1}} = \widehat{C_{0,1}SB_{1,1}}$. Taking into account that $\square C_{0,0}B_{1,0}B_{1,1}C_{0,1}$ of Figure 2 and $\square A_{1,1}A_{0,1}A_{0,2}A_{1,2}$ of Figure 3 are both cyclic plus all the above, including the result that E, D and S are collinear, we concclude that G_1, S, G_2 are collinear.
Finally we show that the line through S and orthogonal to the V-line passes through the center $R_{0,0}$ of the circumcircle and therefore also through the pole $A_{1,1}$:
Since $\widehat{B_{1,0}SB_{1,1}} = \widehat{\phi}$ and $\angle\overrightarrow{C_{0,0}B_{1,0}}\,\overrightarrow{C_{0,1}B_{1,1}} = \widehat{B_{1,0}G_1B_{1,1}} = \widehat{\phi}$, the quadrangle $G_1B_{1,0}B_{1,1}S$ is cyclic. At Figure 2, $\widehat{B_{1,0}G_1B_{1,1}} = \widehat{M_1G_1M_2}$, where M_1 and M_2 are the midpoints of the segments $C_{0,0}B_{1,0}$ and $C_{0,1}B_{1,1}$. Since the triangles $\triangle M_1SB_{1,0}$ and $\triangle M_2SB_{1,1}$ are similar, we have $B_{1,0}S/B_{1,1}S = M_1S/M_2S$ and also $B_{1,0}S/B_{1,1}S = B_{1,0}C_{0,0}/B_{1,1}C_{0,1} = B_{1,0}M_1/B_{1,1}M_2$. Therefore $\triangle B_{1,0}SB_{1,1}$ and $\triangle M_1SM_2$ are similar and also $\widehat{B_{1,0}SB_{1,1}} = \widehat{M_1SM_2}$. So we get $\widehat{M_1SM_2} = \widehat{B_{1,0}SB_{1,1}} = \widehat{\phi}$. From all the above follows that $\square M_1G_1SM_2$ is cyclic and, since $\widehat{G_1M_1R_{0,0}} = \frac{\pi}{2}$, also the pentagon $M_1G_1SM_2R_{0,0}$. $G_1R_{0,0}$ is a diameter of the circumcircle and $\widehat{G_1SR_{0,0}} = \frac{\pi}{2}$. □

All Voronoi hexagons are cyclic. The numbering or their circumcenters $R_{0,0}$, $R_{1,0}$, $R_{1,1}$, ..., as shown in Figure 1, is related to the hexagons: $R_{0,0}$ belongs to the hexagon $B_{0,0}C_{0,0}B_{1,0}C_{1,1}B_{1,1}C_{0,1}$ with the vertex $B_{0,0}$, $R_{1,0}$ to $B_{1,0}C_{1,0}B_{2,0}C_{2,1}B_{2,1}C_{1,1}$ with the vertex $B_{1,0}$, etc. The centres $R_{0,0}$, $R_{1,0}$, $R_{1,1}$ and $R_{0,1}$, form a quadrangle which is similar to the defining quadrangles. Furthermore, the segment $R_{0,0}R_{1,0}$ is parallel to $A_{1,1}A_{2,1}$, because $R_{0,0}R_{1,0}$ is the perpendicular bisector of $B_{1,0}C_{1,1}$, which is the perpendicular bisector of $A_{1,1}A_{2,1}$. Similarly, $R_{1,0}R_{1,1} \parallel A_{2,1}A_{2,2}$, $R_{1,1}R_{0,1} \parallel A_{2,2}A_{1,2}$ and $R_{0,1}R_{1,1} \parallel A_{1,2}A_{1,1}$. The sides of $\square R_{0,0}R_{1,0}R_{1,1}R_{0,1}$ are perpendicular bisectors of the sides of the adjacent Voronoi hexagons; so it is the Voronoi polygon of these hexagons and can be called *VV-quadrangle* ('VV' stands for Voronoi to Voronoi).

As shown in Figure 1, $\square R_{0,0}R_{1,0}R_{1,1}R_{0,1}$ is the VV-quadrangle of the hexagons $B_{0,0}C_{0,0}B_{1,0}$ $C_{1,1}B_{1,1}C_{0,1}$, $B_{1,0}C_{1,0}B_{2,0}C_{2,1}B_{2,1}C_{1,1}$, $B_{1,1}C_{1,1}B_{2,1}C_{2,2}B_{2,2}C_{1,2}$, and $B_{0,1}C_{0,1}B_{1,1}C_{1,2}B_{1,2}C_{0,2}$. Each one of these hexagons is the Voronoi polygon of the relevant four adjacent defining quadrangles, i.e., $B_{0,0}C_{0,0}B_{1,0}C_{1,1}B_{1,1}C_{0,1}$ is the Voronoi polygon of $\square A_{0,0}A_{1,0}A_{1,1}A_{0,1}$, $\square A_{1,0}A_{2,0}A_{2,1}A_{1,1}$, $\square A_{1,1}A_{2,1}A_{2,2}A_{1,2}$, and $\square A_{0,1}A_{1,1}A_{1,2}A_{0,2}$. By (1) we have $\widehat{R_{0,0}SR_{1,0}} = \widehat{\theta}$ and $R_{1,0}S/R_{0,0}S = \lambda$. Since $R_{0,0}R_{1,0} \parallel A_{1,1}A_{2,1}$ and $\widehat{A_{1,1}SA_{2,1}} = \widehat{\theta}$, the points $R_{0,0}$, $A_{1,1}$ and S are collinear as well as $R_{1,0}$, $A_{2,1}$ and S, in order to maintain the ratio λ of similarity of the stretch-rotation with $\square A_{1,1}A_{2,1}A_{2,2}A_{1,2} \mapsto \square A_{2,1}A_{3,1}A_{3,2}A_{2,2}$. Moreover, we notice that $R_{0,0}$ is the circumcenter of the hexagon $B_{0,0}C_{0,0}B_{1,0}C_{1,1}B_{1,1}C_{0,1}$ which has the vertex $A_{1,1}$ in its

interior. So this is the relation between $R_{0,0}$ and $A_{1,1}$ which are collinear with S. Point S can be considered as homothetic centre of the segments $R_{0,0}R_{1,0}$ and $A_{1,1}A_{2,1}$. We summarize:

Lemma 7. *In a Voronoi spiral system, the circumcenters of the hexagons form quadrangles, called VV-quadrangles, which are similar to the defining quadrangles. The VV-quadrangles (like $\square R_{0,0}R_{1,0}R_{1,1}R_{0,1}$ in Figure 1) are the Voronoi polygons of the Voronoi hexagons.*
Each vertex of a VV-quadrangle is related to a specific hexagon as both share in their iterior exactly one vertex of the defining quadrangles. The circumcenter of the hexagon and this unique vertex (e.g., $R_{0,0}$ and $A_{1,1}$ in Figure 1) are collinear with S.

3. General hexagonal spirals and properties

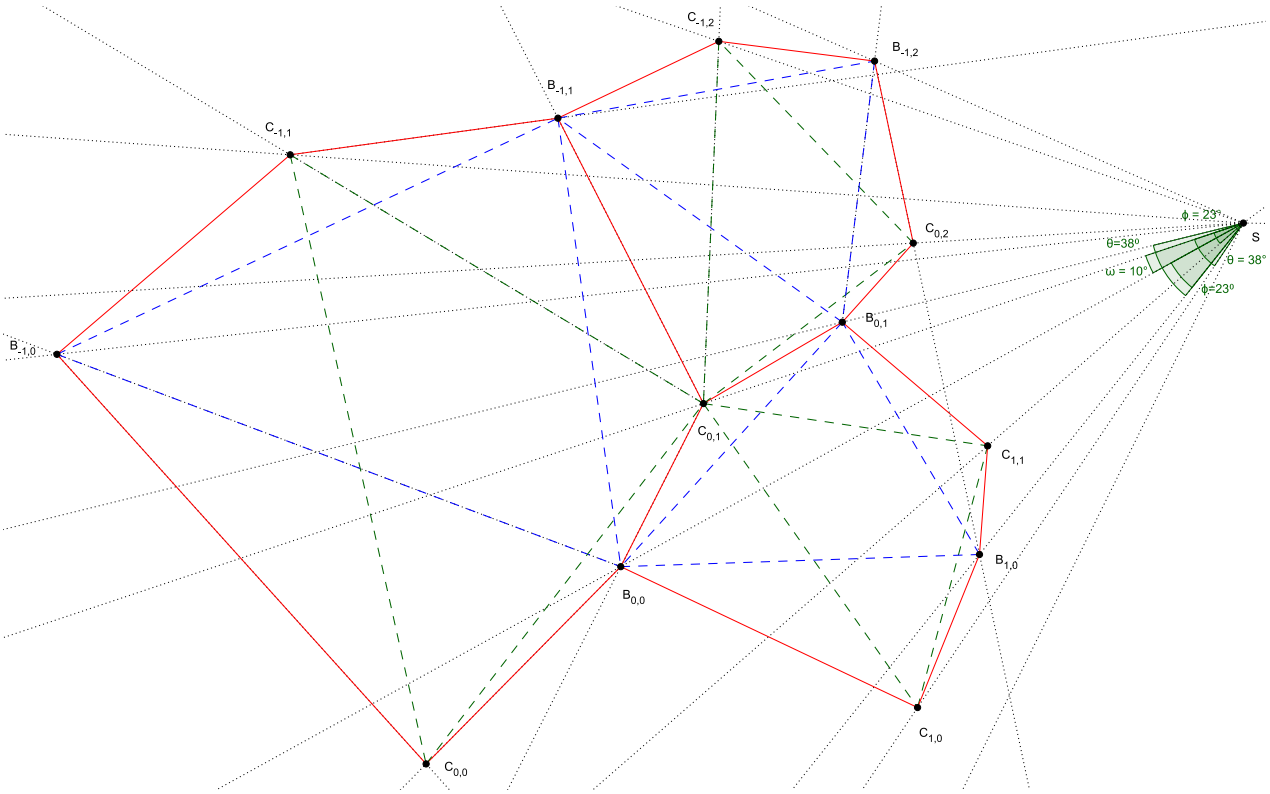

Figure 6: General convex hexagonal spiral system

In Figure 6 the hexagonal spiral system is based on Lemma 6, which is applicable in the general case of hexagonal spiral systems under the following conditions of construction. Under these conditions, we can control the design of any hexagonal system:
a) Given the angles $\widehat{\phi}$ and $\widehat{\theta}$, we can construct the first triangle $\triangle B_{1,0}B_{0,1}B_{0,0}$ by placing its vertices on the rays of angles as we want, as long as the two angles share a common vertex and ray (see Figure 6, S and $SB_{1,0}$, clockwise). The vertices define the similarity ratios as $B_{0,1}S/B_{1,0}S = \lambda$ clockwise, $B_{1,0}S/B_{0,0}S = \kappa$ anticlockwise, and $B_{1,1}S/B_{0,0}S = \alpha$ clockwise. If Eqs. (2) and (3) are valid, the spiral system is closed.
Giving names to the hexagon's vertices is a process which follows Lemma 6 with the relevant triangles and spiral branches. Specifically in the example of Figure 6 two hypotheses were made:

1. For the spiral branches passing through the vertices $B_{i,j}$ and $C_{i,j}$ the index i was chosen to be related in the κ-rotation and similarity ratio ($B_{0,0} \mapsto B_{1,0}$) and the index j to α ($B_{0,0} \mapsto B_{0,1}$).
2. The names of the vertices of the starting hexagon $B_{0,0}C_{0,1}B_{0,1}C_{1,1}B_{1,0}C_{1,0}$ were given in such a way that we do not have negative indices.
These hypotheses can change and another naming process can be applied.

b) Assuming that the hexagon is convex, we place $C_{0,1}$, forming the angle $\widehat{\omega} = \widehat{C_{0,1}SB_{0,0}}$ and we get the ray $SC_{0,1}$. Since each side of the triangle $\triangle C_{0,1}C_{1,0}C_{1,1}$ cuts two sides of the first triangle and according to Lemma 6c1, the sides $C_{0,1}C_{1,0}$ and $B_{0,1}B_{1,0}$ should not intersect and should form an angle $\widehat{\theta}$ with S, we define the angle $\widehat{\theta}$ with one of its sides passing from vertex $C_{0,1}$ and point S, anticlockwise (in order to cut the other two sides of $\triangle B_{1,0}B_{0,1}C_{0,0}$). As a next step we define $C_{1,0}$ on the other side of the angle, taking care that $\lambda = C_{0,1}S/C_{1,0}S$ in order to have the same ratio of similarity and the same orientation in the two spiral branches (see [3]). We continue the next step by defining the angle $(\widehat{\theta} - \widehat{\phi})$ with one of its sides passing from vertex $C_{1,0}$ and point S, defining also $C_{1,1}$ on the other side of the angle, taking care that $\alpha = C_{1,1}S/C_{1,0}S$ in order to have the same ratio of similarity and orientation in the two spiral branches, so $\triangle C_{0,1}C_{1,0}C_{1,1}$ is formed.
From these triangles, the rotation of spiral branches and ratios of similarity, we get $\lambda = B_{0,1}S/B_{1,0}S = C_{0,1}S/C_{1,0}S$ and $\widehat{C_{0,1}SC_{1,0}} = \widehat{B_{0,1}SB_{1,0}} = \widehat{\theta}$. Therefore, from the similarity of the relevant triangles, $C_{0,1}B_{0,1}/C_{1,0}B_{1,0} = \lambda$. Similarly we can obtain $C_{1,1}B_{1,0}/C_{0,1}B_{0,0} = \kappa$ and $C_{1,1}B_{0,1}/C_{1,0}B_{0,0} = \alpha$.
In order to construct the next hexagon $B_{0,0}C_{0,0}B_{-1,0}C_{-1,1}B_{-1,1}C_{0,1}$, the point $C_{-1,1}$ is defined by rotating the segment $C_{0,1}C_{1,1}$ anticlockwise by an angle $\pi - \widehat{\theta}$ about the vertex $C_{0,1}$ and angle $\widehat{C_{-1,1}SC_{0,1}} = \widehat{\theta}$; similarly point $B_{-1,0}$ is defined. The point $C_{0,0}$ is defined by the angles $\widehat{B_{0,0}B_{-1,0}C_{0,0}} = \widehat{B_{1,0}B_{0,0}C_{1,0}}$ and $\widehat{B_{-1,0}B_{0,0}C_{0,0}} = \widehat{B_{0,0}B_{1,0}C_{1,0}}$, and similarly point $B_{-1,1}$. Any other hexagon can be constructed in a similar way. So the spiral branches equivalent to Lemmas 6c1, 6c2 and 6c3 are as shown in Figure 6:
a) $C_{-1,2}C_{0,1}C_{1,0}\ldots$ and $B_{-1,2}B_{0,1}B_{1,0}\ldots$; the vertices of each segment form $\widehat{\theta}$ with S due to the λ-stretch-rotation.
b) $C_{0,0}C_{0,1}C_{0,2}\ldots$ and $B_{-1,0}B_{-1,1}B_{-1,2}\ldots$ forming then angle $\widehat{\theta} - \widehat{\phi}$ with S, due to the α-stretch-rotation.
c) $C_{-1,1}C_{0,1}C_{1,1}\ldots$ and $B_{-1,0}B_{0,0}B_{1,0}\ldots$, forming $\widehat{\phi}$ with S, according to the κ-stretch-rotation.

As in the case of Voronoi hexagons, the similarity ratios κ, λ, α are related to spiral branches of which any two of them can co-rotate and the third contra-rotate or any two of them contra-rotate and the third co-rotate or three of them co-rotate. Also in Figure 6 we have $\alpha = \kappa\lambda$, since $B_{0,1}S/B_{0,0}S = \alpha$, $B_{0,1}S/B_{1,0}S = \lambda$, $B_{1,0}S/B_{0,0}S = \kappa$ and $\widehat{B_{0,0}SB_{0,1}} = \widehat{C_{1,0}SC_{1,1}} = \widehat{\theta} - \widehat{\phi}$. Similar to Lemma 6d, the combination of vertices of general hexagons can form two types of quadrangles (note $\square C_{0,0}C_{-1,1}C_{0,1}C_{1,0}$ and $\square B_{0,0}B_{-1,1}B_{0,1}B_{1,0}$ in Figure 6). Each type is a defining quadrangle of a spiral system. The method of defining the hexagon is the same for concave hexagons. We conclude:

Theorem 3. *The construction of the starting hexagon $B_{0,0}C_{0,1}B_{0,1}C_{1,1}B_{1,0}C_{1,0}$ of a general hexagonal spiral system (see Figure 6) is based on the position of S, on the angles $\widehat{\phi}$ and $\widehat{\theta}$, one the vertices of $\triangle B_{0,0}B_{1,0}B_{0,1}$ (similarity ratios and rotations of κ-, λ- and α-branches), on $\widehat{\omega} = \widehat{C_{0,1}SB_{0,0}}$ plus point $C_{0,1}$. The other hexagons follow by Lemma 6.*

4. Spiral systems beyond hexagonal spirals

Let $A_0A_1A_2\dots A_{n-1}$ be a convex polygon with n sides and interior angles and let R be a point in its interior. Each triangle, which is formed by two consecutive vertices and point R, has the following angles: $\widehat{RA_iA_{i+1}}$, $\widehat{A_iA_{i+1}R}$ and $\widehat{A_{i+1}RA_i}$ ($0 \le i \le n-2$ and $\widehat{RA_iA_{i+1}} + \widehat{A_iA_{i+1}R} + \widehat{A_{i+1}RA_i} = \pi$). The sum of all interior angles of the polygon is

$$\begin{aligned} S_a &= \widehat{RA_0A_1} + \widehat{A_0A_1R} + \widehat{A_1RA_0} + \widehat{RA_1A_2} + \widehat{A_1A_2R} + \widehat{A_2RA_1} + \dots \\ &\quad + \widehat{RA_{n-1}A_0} + \widehat{A_{n-1}A_0R} + \widehat{A_0RA_{n-1}} \\ &= n\pi - (\widehat{A_1RA_0} + \widehat{A_2RA_1} + \dots + \widehat{A_0RA_{n-1}}) = (n-2)\pi. \end{aligned}$$

The same formula exists for non convex polygons, following the same proof. The average size of each angle at the polygon must be $A_a = S_a/n$.
Each n-polygon spiral system has N polygons/N angles per vertex. So for all spiral systems $n = N.p$, $p \in \mathbb{N}$, plus the sum of angles at each vertex of the system must be 2π. Hence average size of a polygon angle is $A_v = 2\pi/N$, and we get:

Remark 1. $S_a = (n-2)\pi$ and $n = N.p$, $p \in N$.

Remark 2. $A_a = S_a/n$ and $A_v = 2\pi/N$.

For $n = 8$ and for $N = 4$, we get from Remark 2 that $A_a = \frac{3\pi}{4}$ and $A_v = \frac{2\pi}{3}$, so no solution exists. If N increases, then A_v becomes smaller, so again no solution. When n increases, A_a increases too, since $A_a = S_a/n = (n-2)\pi/n = \pi - 2\pi/n$, so no solution exists for $n > 6$, since $A_v = \frac{2\pi}{3}$ for $N = 3$ and less for $N > 3$. For $n = 6$ and for $N = 3$, we get from Remark 2 that $A_a = \frac{2\pi}{3}$ and $A_v = \frac{2\pi}{3}$, so no solution exists. For $n = 5$ there is no solution for $N \in [3, 4, 5]$ because of Remark 1 when $N = 3$ and $N = 4$, also $A_a = \frac{3\pi}{5}$ and $A_v = \frac{2\pi}{5}$ when $N = 5$. However, when $n = 6$, $N = 3$ and three consecutive vertices become collinear or three consecutive vertices form a zero angle, we have a pentagon spiral system (with six vertices per pentagon). Similarly, for $n = 3$ there is no solution for $N \in [3, 4]$ because of Remarks 1 and 2, since 4 does not divide 3 in case of $N = 4$, also $A_a = \frac{\pi}{3}$ and $A_v = \frac{2\pi}{3}$ in case of $N = 3$. However, when $n = 4$, $N = 4$ and three consecutive vertices become collinear, we have a triangular spiral system (with four vertices per triangle), as seen in [3], [5] and [7]. Similarly, there is no solution for $n = 7$ and $N \in [3, 4, 5, 6, 7]$ for obvious reasons. From all the above, we get

Theorem 4. *Spiral systems can have either 4 or 6 vertices per polygon, forming triangles, quadrangles (4 vertices), pentagons and hexagons (6 vertices).*

5. Appendix

In Figure 4, by applying the Law of Sines, from $\triangle A_{0,2}A_{0,1}E$, we have

$$\frac{\sin\widehat{\phi}}{A_{0,2}A_{0,1}} = \frac{\sin\widehat{\tau_1}}{EA_{0,1}} = \frac{\sin\widehat{\tau_2}}{EA_{0,2}}.$$

Similarly from $\triangle A_{1,1}A_{1,2}E$:

$$\frac{\sin\widehat{\phi}}{A_{1,2}A_{1,1}} = \frac{\sin\widehat{\omega}}{EA_{1,2}} = \frac{\sin\widehat{\tau_3}}{EA_{1,1}},$$

and, since the branches co-rotate,

$$\kappa = \frac{A_{1,2}A_{0,2}}{A_{1,1}A_{0,1}} < 1, \quad \lambda = \frac{A_{0,1}A_{0,2}}{A_{1,1}A_{1,2}} < 1 \implies \frac{1}{A_{0,1}A_{0,2}} > \frac{1}{A_{1,1}A_{1,2}}.$$

From the above relation and from the two applications of the Law of Sines, we get

$$\frac{\sin\widehat{\tau_1}}{EA_{0,1}} > \frac{\sin\widehat{\omega}}{EA_{1,2}}, \tag{i}$$

$$\frac{\sin\widehat{\tau_2}}{EA_{0,2}} > \frac{\sin\widehat{\tau_3}}{EA_{1,1}}. \tag{ii}$$

If we assume $EA_{0,1} > EA_{1,2}$, then from (i) we get $\sin\widehat{\tau_1} > \sin\widehat{\omega}$, otherwise, if $EA_{0,1} < EA_{1,2}$, from (ii) we get $\sin\widehat{\tau_2} > \sin\widehat{\tau_3}$. So it is impossible to have a cyclic $\square A_{0,0}A_{0,1}A_{1,1}A_{1,0}$, as this would require $\sin\widehat{\tau_1} = \sin\widehat{\omega}$ and $\sin\widehat{\tau_2} = \sin\widehat{\tau_3}$, provided that the branches co-rotate.

References

[1] H.S.M. Coxeter: *Introduction to Geometry*. 2nd ed., John Wiley and Sons, Inc., 1989.

[2] R.V. Jean: *Phyllotaxis, a systemic study in plant morphogenesis*. Cambridge University Press, 1994.

[3] K. Myrianthis: *Geometry and Design of Equiangular Spirals*. In Ch. Ashbacher (ed.): *Topics in Recreational Mathematics 1/2016*, pp. 68–102..

[4] P.S. Stevens: *Patterns in Nature*. Little, Brown and Comp., Boston, Toronto 1974, 1994.

[5] T. Sushida, A. Hizume, Y. Yamagishi: *Triangular Spiral Tilings*. J. Phys. A **45**, 235203 (2012).

[6] A. Vigneron: *Voronoi Diagrams and Delaunay Triangulations*. Lecture 11 of CS 372: Computational Geometry, King Abdullah Univ. of Science and Technology, Nov. 2012, `https://algo.kaust.edu.sa/documents/cs372l11.pdf`.

[7] Y. Yamagishi, T. Sushida, A. Hizume: *Voronoi Spiral Tilings*. Nonlinearity **28**/4, 1077—1102 (2015).

Received December 29, 2016; final form October 18, 2017